Roles of Clouds and Aerosols in Climate Change Processes

T. Nakajima

(University of Tokyo)

Roles of Clouds and Aerosols in Climate Change Processes

Teruyuki Nakajima
Center for Climate System Research, University of Tokyo
(teruyuki@ccsr.u-tokyo.ac.jp)

1. Introduction

Extensive efforts have been paid in the last decade for understanding the mechanism of global change processes due to anthropogenic increase of greenhose gases and air pollutants. Two observations have been recognized recentely as significant in the problem. One is the recognition that global warming simulations by climate models systematically overestimate the observed record of surface temperature in the last one hundred years. A cooling effect of anthropogenic aerosols has been regarded as one of main causes for the discrepancies (Mitchell et al., 1995).

Another observation is that a number of satellite remote sensing studies have provided examples of global scale signatures of aerosols and clouds modulating the earth's climate system. NOAA operational aerosol products have shown a large stratospheric aerosol development (Stowe et al., 1992), Saharan soil-derived aerosols and South African smokes due to biomass burning, and TOMS detected a large amount of biomass burning aerosols over land areas (Herman, 1995). Han et al. (1994) have found a global scale change in the cloud effective particle radius over continental regions, that may be a results of interaction of clouds with dense continental aerosols. Ramanathan and Collins (1991) have segested that the tropical sea surface temperature (SST) can be stabilized by SST-cirrus coupling.

Our next step to take with the above mentioned significan heritage will be to evaluate more quantitatively the observed phenomena with more data analyses and more realistic modelling . In this paper we will discuss the role of aerosols and clouds in climate change processes with our analyses of satellite data.

2. An aerosol microphysics retrieval

Figure 1 shows are ten day composites of the aerosol optical thickness and Ångström exponent as retrieved from NOAA/AVHRR for July, 1988 data set. The two channel algorithm of Nakajima et al. (1996) and Higurashi and Nakajima (1996) with channel-1 and -2 radiances of AVHRR have been used for the analyses. The figure shows that soil-derived aerosols over oceans off Saharan and Middle East arid areas are main contributors of shortwave radiative forcing of aerosols. Another interesting feature in Fig. 1 is that although optically thin the regions around large cities such as New York city are detected as a region with large Ångstöm exponent values. This suggests that small aerosol particles are generated by active gas-to-particle conversion process around those regions due to air pollution, although it is possible to detect mistakenly turbid water around large rivers as aerosols. If we compare our optical thickenss values with those from the NOAA operational algorithm, it is found that the NOAA optical thickness is smaller than

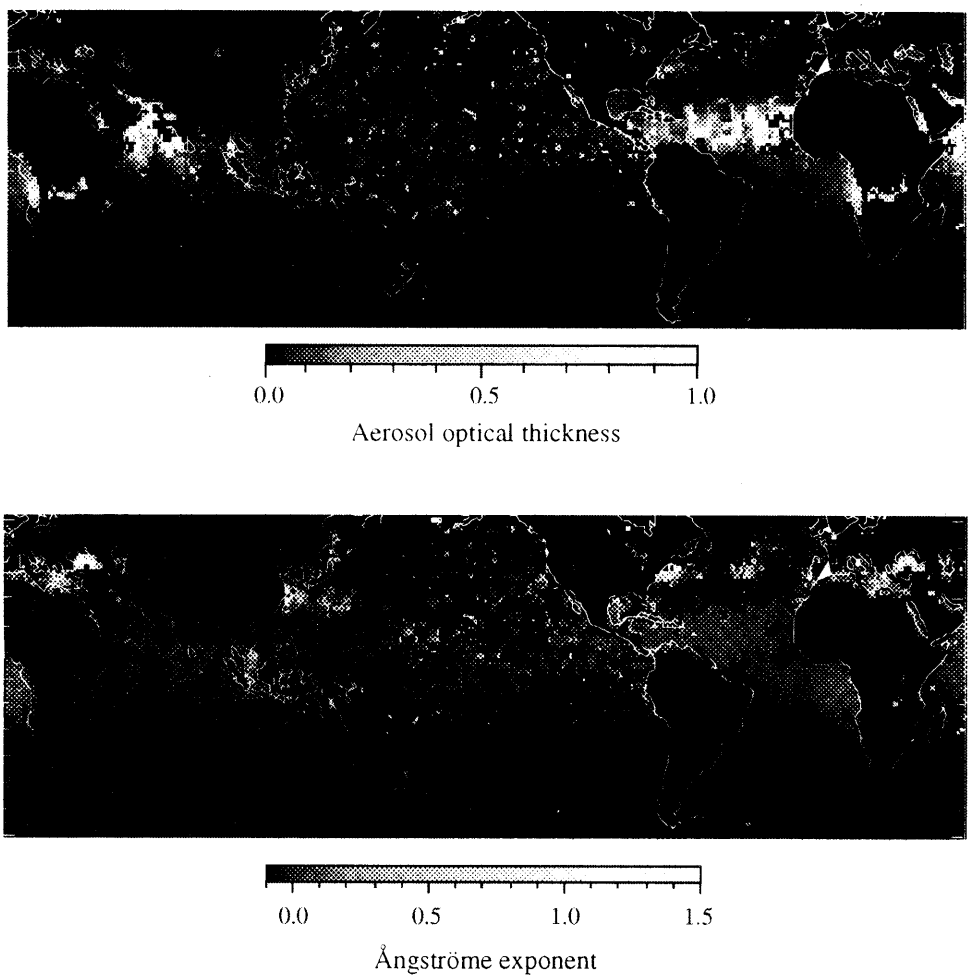

Fig. 1 Aerosol optical thickness and Ångström exponent as retrieved from a two channel algorithm with NOAA/AVHRR radiometer data. Ten days composits of July, 1988.

our resutls by factor of 2 in some regions. The two algorithms are different in several points. The NOAA algorithm is one channel algorithm whereas ours is of two channels. We have adopted absorption aerosols with more realistics sea surface boundery condition than NOAA algorithm, which is generated by a comprehensive radiative transfer package *R-star*, an assemble of algorithms of Nakajima and Tanaka (1983, 1986, 1988) and Lowtran-7 gas absorption model. Anyway the estimation of direct radiative forcing of aerosols will change significantly with these results if the difference is realistic. Especially the radiative forcing at the earth's surface will have a large effect.

3. An cloud microphysics retrieval

Figure 2 shows ten day composites of the cloud optical thickness and effective particle radius fields with January, 1988 data. For the analyses, we have modified the three channel algorithm of Nakajima and Nakajima (1995) for global data analyses with channel-1, -3, and -4 radiances of AVHRR. It is found from Fig. 2 that the effective particle radius of warm clouds with cloud top temperature larger than 270K decreases over continental regions. This finding is similar

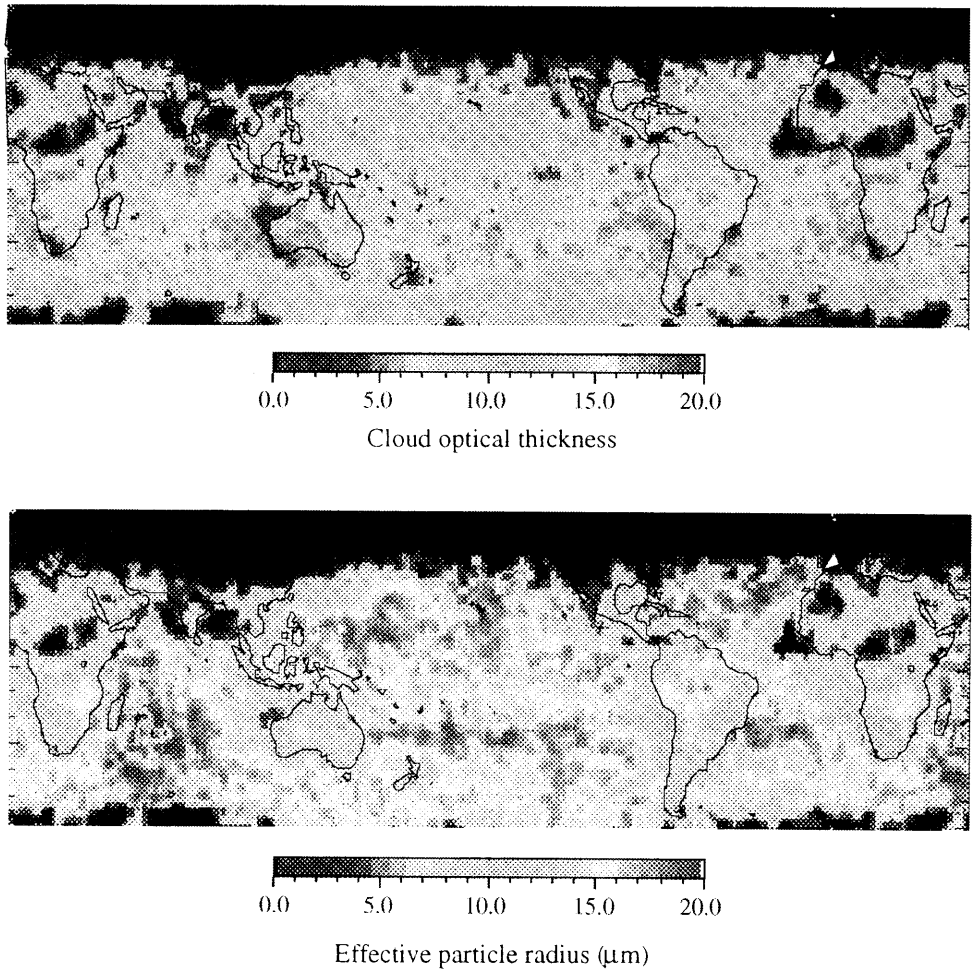

Fig. 2 Cloud optical thickness and effective particle radius as retrieved from a three channel algorithm of NOAA/AVHRR radiometer data. Ten days composits of January, 1988.

to Han et al. (1994). However the average values of effective particle radius are 10 μm and 18 μm over land and ocean areas, respectively, and are systematically larger by 2 μm than those of Han et al. Another important feature in Fig. 2 is that there seems no noticeable increase in the cloud optical thickness around the peripherals of large continents. Albrecht (1989) and Nakajima and Nakajima (1995) have pointed out that the cloud optical thickness will increase significantly if the cloud layer is rich in drizzle particles. A cloud-aerosol interaction will reduce the cloud particle size and quench the drizzling from the cloud layer. Although not shown in a figure, upper clouds did not show a significant change in particle size over continental regions. It may be suggested, therefore, that the cloud particle reduction is a special phenomenon near the surface.

It is clear by these results that more data analyses will be needed to lead the final conclusion for this issue.

4. Cloud statistics important for the space lidar mission

The discussion in the preceding sections shows that the aerosol and cloud remote sensing are necessary for further assessment of aerosol and cloud effects on the earth's climate formation.

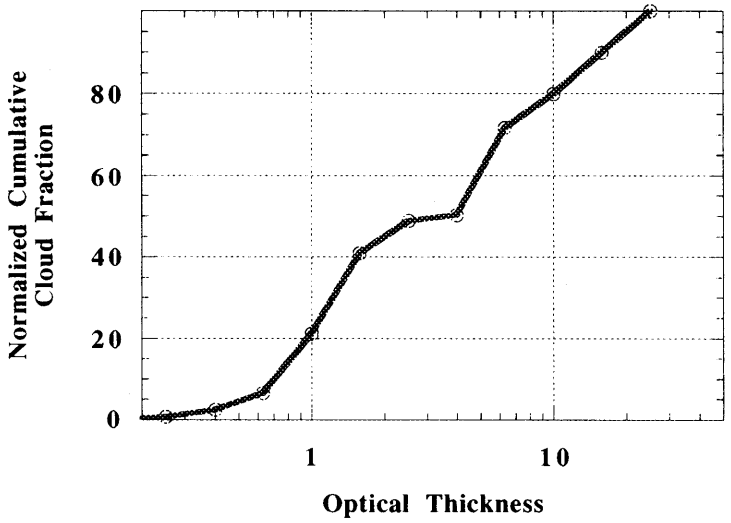

Fig. 3 Normalized cumulative cloud fraction as a function of the cloud optical thickeness, generated from ISCCP-C2 cloud statistics of 1986.

A spaceborne lidar will give us another independent constraint for the discussion. The optical thicknesses of aerosols and clouds can be retrieved with the space lidar system which can be compared with retrievals from the existing passive radiometer techniques. With such comparisons the Ångstöm exponent and/or absorption index of aerosols can be retrieved with better accuracy.

Figure 3 shows the normalized cumulative cloud fraction as a function of the cloud ooptical thickness generated from ISCCP-C2 cloud statistics of 1986. According to the ISCCP statistics a space lidar can detect 40 to 50% of clouds if the detection limit is assumed as an optical thickness around 1-3. A spaceborne lidar system is, therefore, enough useful to produce an important data set of aerosol and cloud statistics that are independent from the existing statistics which are mainly generated from passive radiometers. It should be noted that the results of the re-analyses of ISCCP are much different from the original statistics, especially for upper level clouds. Cloud fraction of cirrus/cirrostratus clouds have increased from 14.2% to 19.6% due to an improvement of the cirrus cloud detection threshould. It is also noteworthy to find from Fig. 1 thata the optical thickness of aerosols is as large as 1 for significantly large areas of the globe.

5. A conclusion

We have shown by the discussions in the preceding sections that the recent satellite retrievals still have a large difference among them in the estimation of the optical thickness and particle size depending on retrieval algorithms and adopted data sets, even though those retrievals are clearly showing significant signatures of aerosols and clouds affecting the earth's climate formation. We will need more data analyses and careful discussion to lead clearer images on the role of aerosols and clouds in climate change processes.

References

Albrecht, B. A., 1989: Aerosols, cloud microphysics, and fractional cloudiness. *Science*, **245**, 1227-1230.

Han, Q., W. B. Rossow, and A.A. Lacis, 1994: Near-global survey of effective droplet radii in liquid water clouds using ISCCP data. *J. Climate*, **7**, 465-497.

Harman, J., 1995: A discussion on the TOMS global analyses of aerosols. Private communication.

Higurashi, A., and T. Nakajima, 1996: An analysis of radiative fields in a coupled atmosphere-ocean system. *Proc. Int. Radiation Symp. '96*, Fairbanks, August, 1996.

Mitchell,J.F.B., T.C.Johns, J.M.Gregory, and S.F.B.Tett, 1995: Climate response to increasing levels of greenhouse gases and sulphate aerosols. *Nature*, **376**, 501-504.

Nakajima, T., and M. Tanaka, 1983, Effect of wind-generated waves on the transfer of solar radiation in the atmosphere-ocean system. *J. Quant. Spectrosc. Radiat. Transfer*, **29**, 521-537.

Nakajima, T., and M. Tanaka, 1986, Matrix formulations for the transfer of solar radiation in a plane-parallel scattering atmosphere. *J. Quant. Spectrosc. Radiat. Transfer*, **35**, 13-21.

Nakajima, T., and M. Tanaka, 1988, Algorithms for radiative intensity calculations in moderately thick atmospheres using a truncation approximation. *J. Quant. Spectrosc. Radiat. Transfer*, **40**, 51-69.

Nakajima, T., and A. Higurashi, 1996: AVHRR Remote Sensing of Aerosol Optical Properties in the Persian Gulf Region, the Summer of 1991. Accepted by *J. Geophys. Res.*

Nakajima, T. Y., and T. Nakajima, 1995, Wide-area determination of cloud microphysical properties from NOAA AVHRR measurements for FIRE and ASTEX regions. *J. Atmos. Sci.*, **52**, 4043-4059.

Ramanathan, V., and W. Collins, 1991: Thermodynamic regulation of ocean warming by cirrus clouds deduced from observations of the 1987 El Nino. *Nature*, **351**, 27-32.

Stowe, L. L., R. M. Carey, and P. P. Pellegrino, 1992: Monitoring the Mt. Pinatubo aerosol layer with NOAA/11 AVHRR data. *Geophys. Res. Lett.*, **19**, 159-162.

Wetherald, R. T., and S. Manabe, 1988: Cloud feedback processes in a general circulation model. *J. Atmos. Sci.*, **45**, 1397-1415.

Roles of Clouds and Aerosols in Climate Change Processes

Teruyuki Nakajima
Center for Climate System Research, University of Tokyo
(teruyuki@ccsr.u-tokyo.ac.jp)

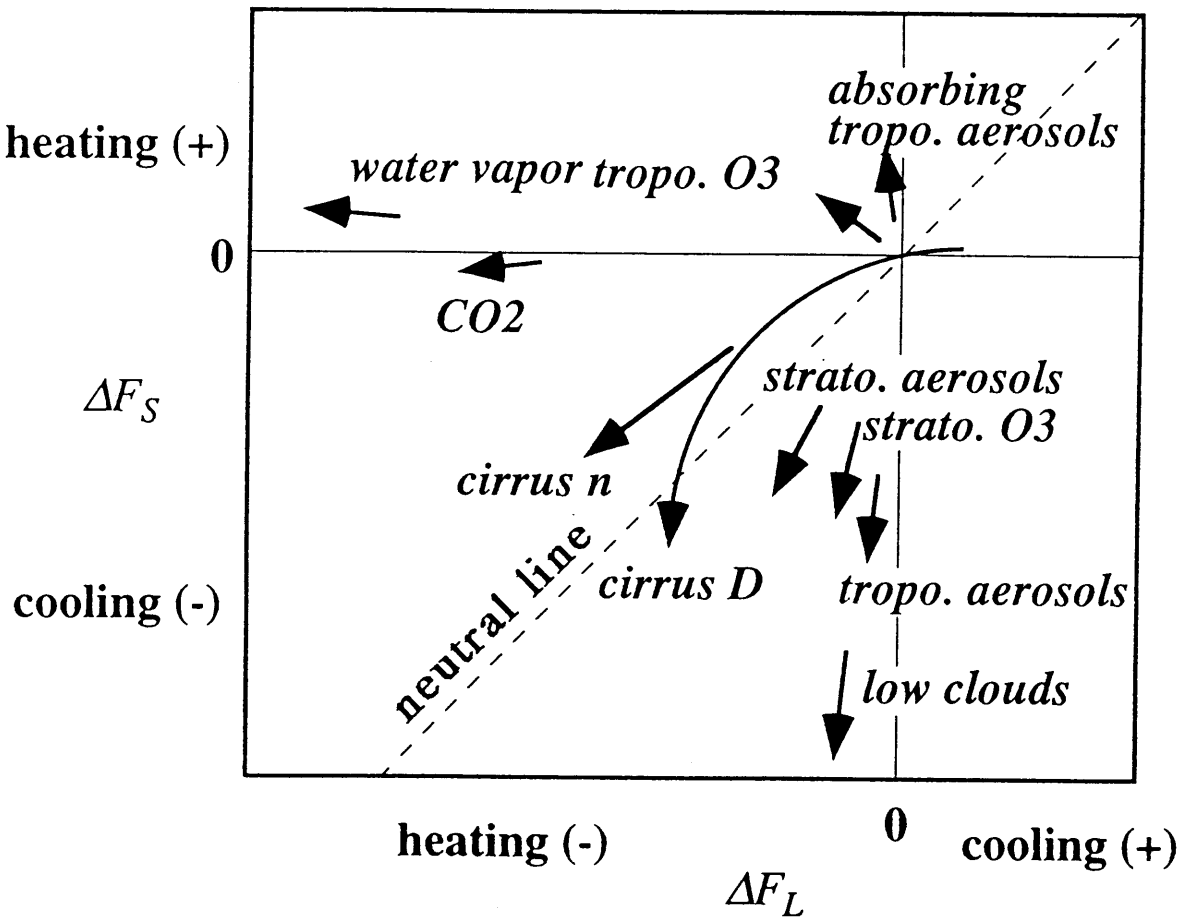

Climate issues related with cloud and aerosol systems

* Cloud change due to global warming?

- Cloud radiative forcing

$$\Delta T = \gamma\lambda\,\Delta F \qquad \lambda \approx 1\ KW^{-1}m^2, \quad \gamma = 0.5$$

$$\Delta F_s = -3.4\ Wm^{-2} \quad for \quad \Delta\alpha = +0.01 \quad (e.g., \Delta n = 0.017, \Delta\tau = 0.076)$$

$$\alpha = 0.05 + n\left(1 - \frac{4}{4.3 + 0.45\tau_c}\right) \qquad \alpha = 0.3,\ n = 0.66 \rightarrow \tau_c = 5.1$$

ISCCP: $n = 0.66,\ \tau_c = 7.0$

$$\Delta F_L = +4\ Wm^{-2} \qquad for \quad 2 \times CO_2$$

$$\Delta F_L = +1.3\,Wm^{-2} \quad at\ TOA, \quad for\ \Delta z = +1km$$

$$= -6.6\,Wm^{-2} \quad at\ SRF \quad (23.9\,Wm^{-2} \quad with\ 6\,K\,km^{-1})$$

	1986		1990	
	Stage C2	Stage D2	Stage C2	Stage D2
North polar cloud amount (%)				
Winter	54.9	70.2	56.7	71.2
Spring	44.4	65.4	49.8	72.2
Summer	54.7	68.2	53.5	66.9
Autumn	53.9	69.4	54.7	69.6
South polar cloud amount (%)				
Winter	57.5	70.1	55.4	69.3
Spring	50.1	66.6	49.4	68.4
Summer	47.6	67.8	49.1	71.2
Autumn	55.1	69.8	56.2	72.2
Ocean cloud amount (%)	71.2	73.0	68.6	71.3
Land cloud amount (%)	46.0	58.8	45.0	58.6
Global cloud amount (%)	63.4	68.6	61.3	67.3
Total optical thickness	8.0	4.3	6.8	4.5
Total pressure (mb)	600	580	580	576
Cirrus/cirrostratus amount (%)	14.2	19.6	15.9	19.0
Cirrus/cirrostratus optical thickness	4.1	3.2	4.0	3.6
Cirrus/cirrostratus pressure (mb)	289	258	281	265

Table 1. Comparison of C2 and D2 cloud results for 1986 and 1990

- **Climate sensitivities**

$(WV, LWP, P; T_S, \Gamma, D)$

WV>Ice Albedo>Clouds>Lapse rate

Cloud overlapping effect is large

$$\tau_c/2 + \tau_c/2 \rightarrow \alpha_R = 0.33$$

*** Model cloud height distribution has less freedom than nature for convective clouds, cirrus clouds**

-> Statistics of cloud overlapping

High cloud fraction(%)

T21L20 DJF mean

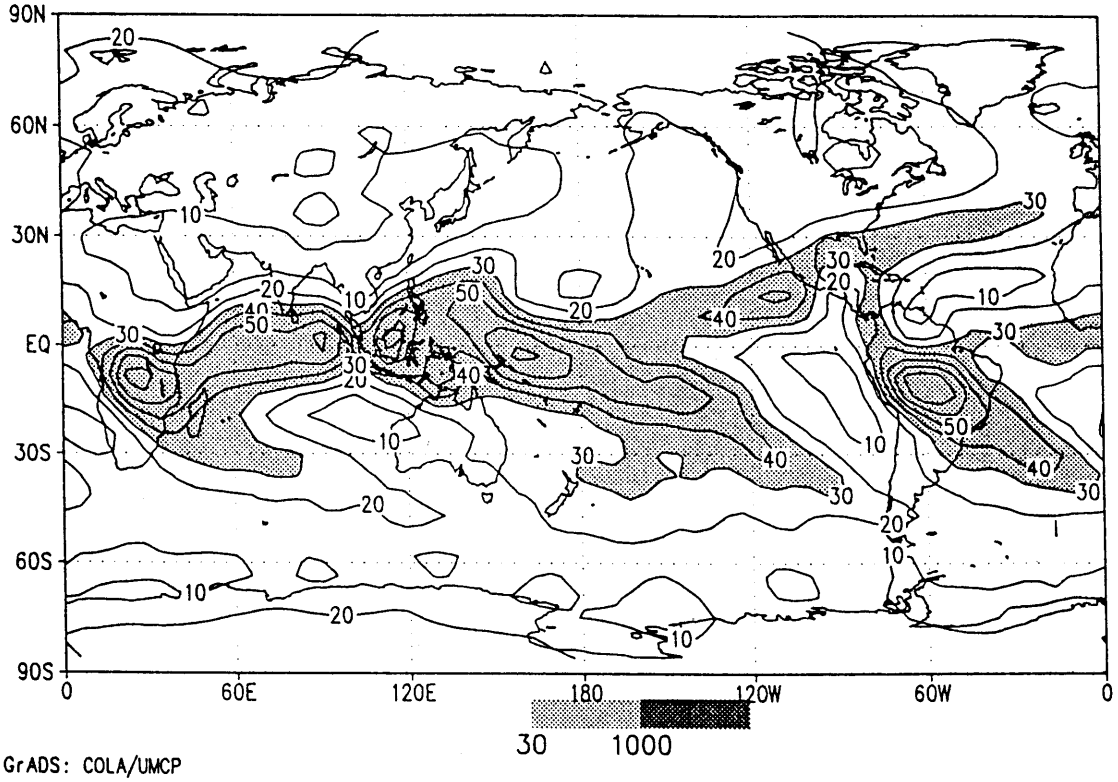

GrADS: COLA/UMCP

High cloud fraction(%)

ISCCP

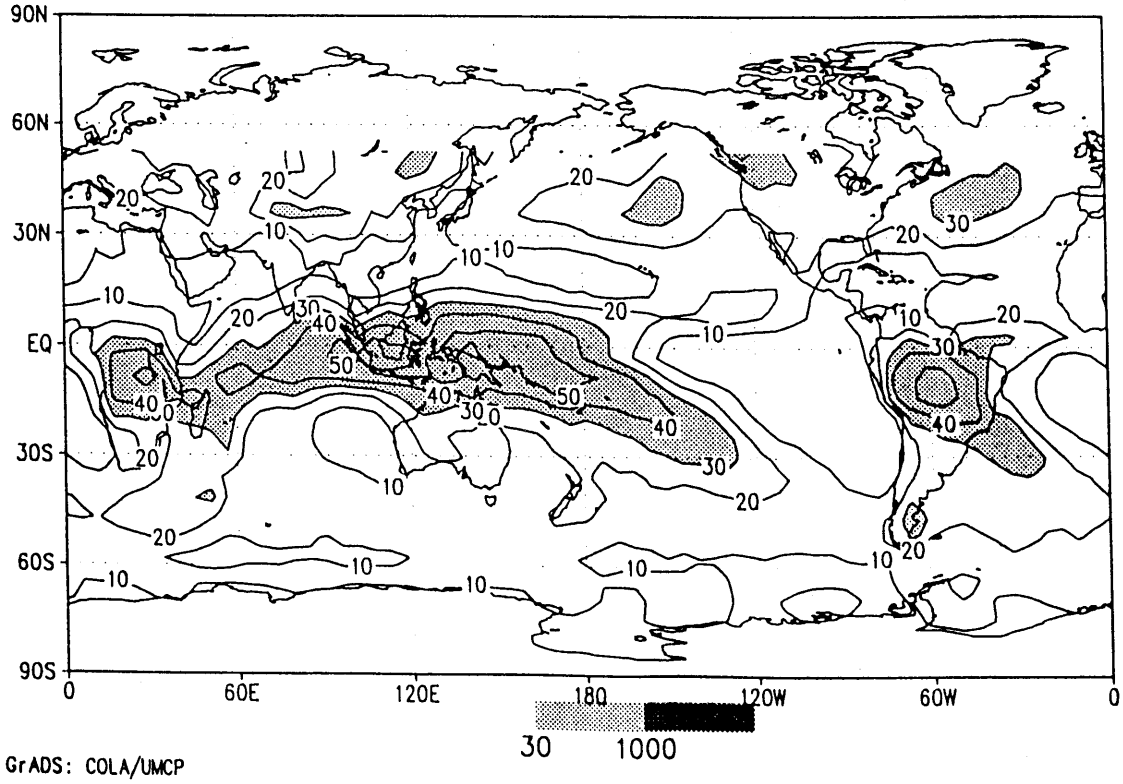

GrADS: COLA/UMCP

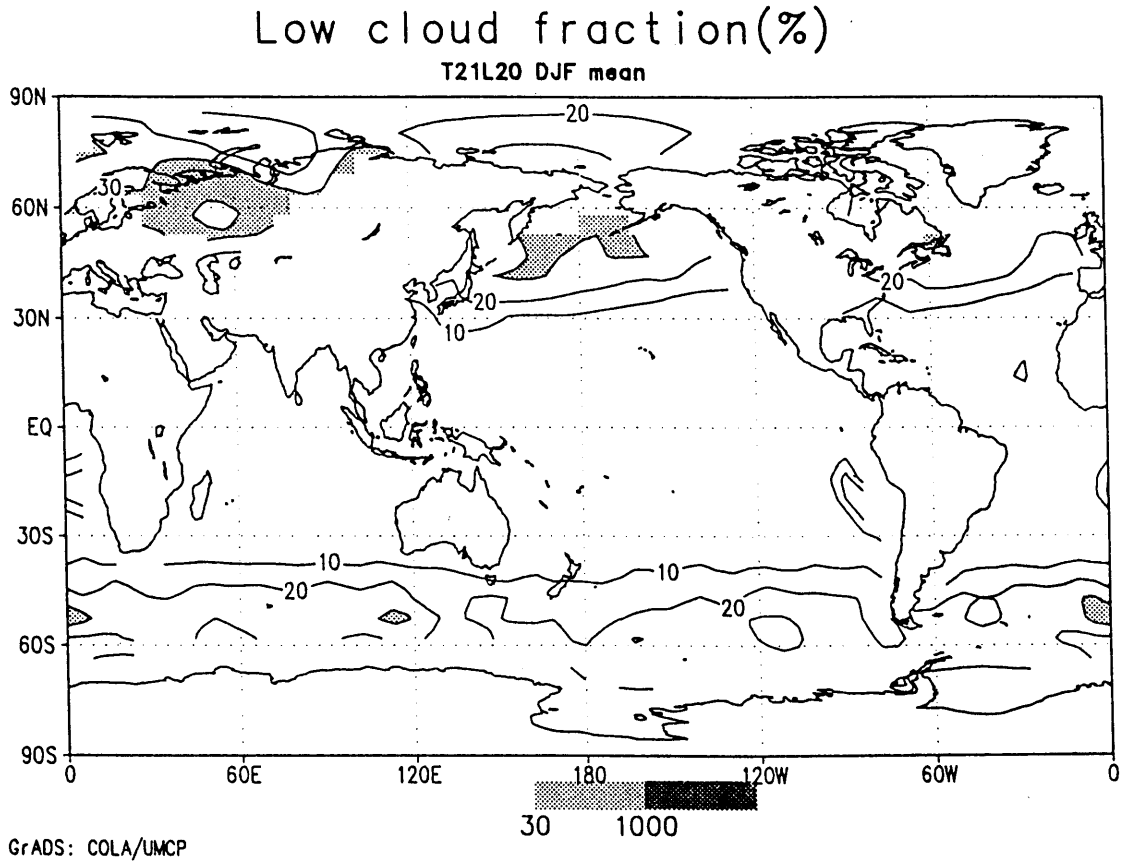
Low cloud fraction(%)
T21L20 DJF mean
90N
60N
30N
EQ
30S
60S
90S
0
60E
120E
180
120W
60W
0
20
30
10
30
1000
GrADS: COLA/UMCP

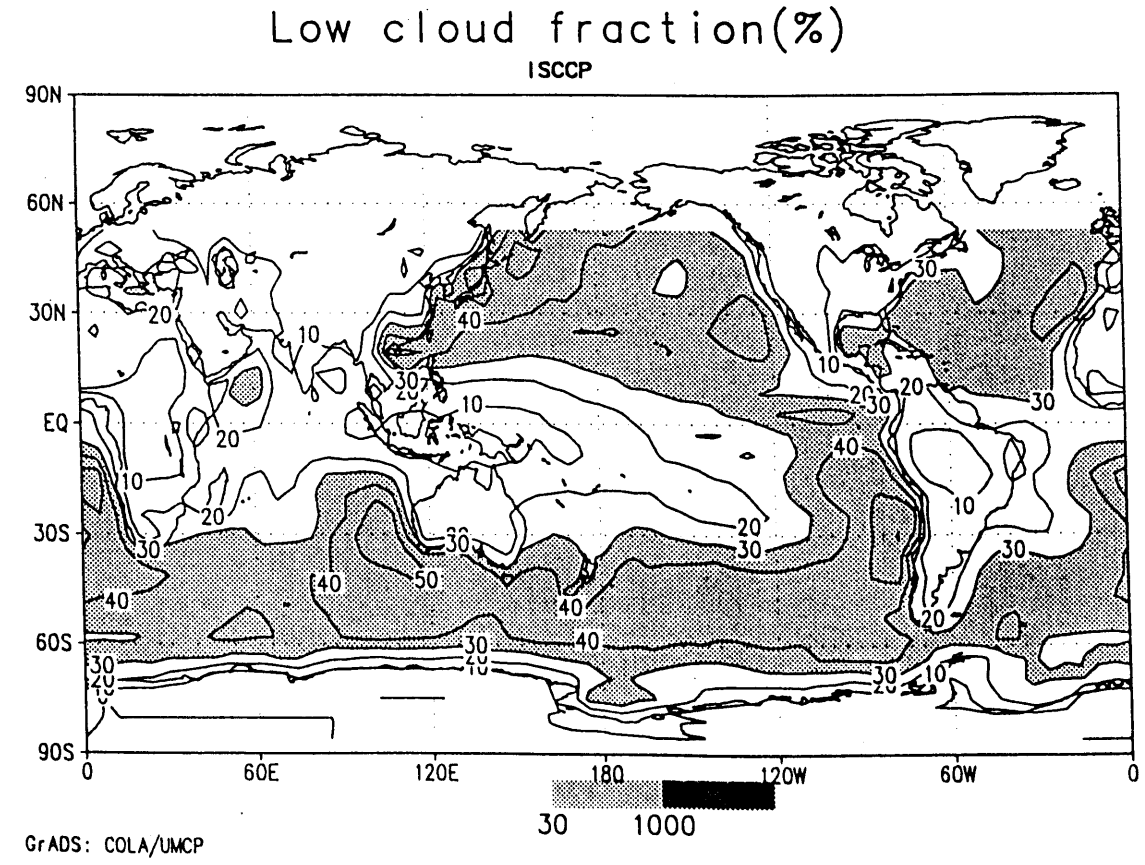
Low cloud fraction(%)
ISCCP
90N
60N
30N
EQ
30S
60S
90S
0
60E
120E
180
120W
60W
0
10
20
30
40
50
30
1000
GrADS: COLA/UMCP

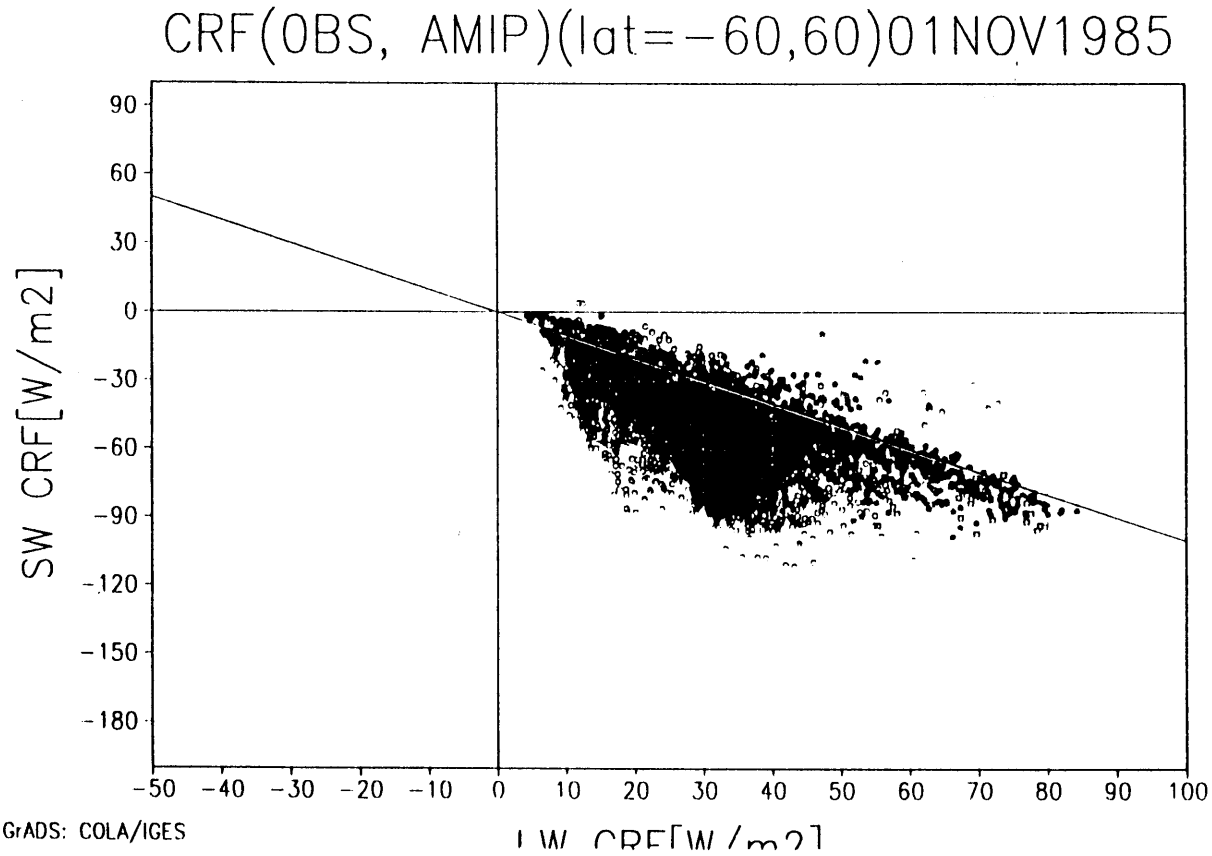
CRF(OBS, AMIP)(lat=-60,60)01NOV1985
SW CRF[W/m2]
90
60
30
0
-30
-60
-90
-120
-150
-180
-50 -40 -30 -20 -10 0 10 20 30 40 50 60 70 80 90 100
GrADS: COLA/IGES

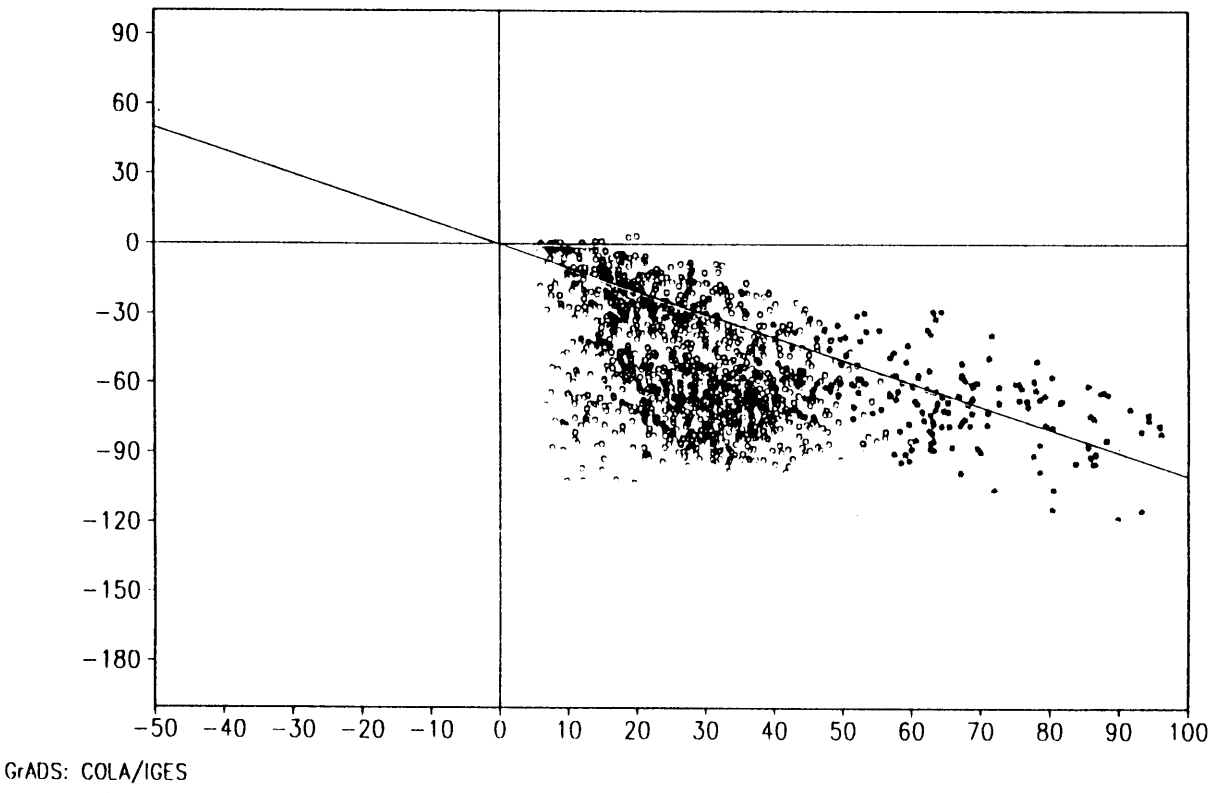
90
60
30
0
-30
-60
-90
-120
-150
-180
-50 -40 -30 -20 -10 0 10 20 30 40 50 60 70 80 90 100
GrADS: COLA/IGES

Tropospheric Aerosols ; Magnitude of Forcing ?

○ 対流圏エアロゾルの影響：その大きさは？

Direct effect Charlson et al. (92)

・直接効果：$\approx -1 W/m^2$ (Natural: $\approx -10 W/m^2$)

- land aerosols; desert aerosols
- soot particles (BC/TP = 10%)

$\omega \leq 0.95$

DMS ⟷ water vapor ⟷ T_s

南北差

Indirect effect

・間接効果：$-0.3 W/m^2 \sim -0.9 W/m^2$???

>> Twomey effect (0.1 K → 0.5K?)

cleaning effect

Charlson et al. (92)

$N/N_0 = 1.15$

$\rightarrow \Delta F_{ind.} = -1.0$ w/m

・CZCS, AVHRR, TOMS (aerosol absorption)

・Future：OCTS, SeaWiFS, MODIS, GLI

$\Delta F_R = -1.5$ NH

-1.0 SH

(UK Met. Office)

・Upscatter fraction $b = 0.3 + 0.074 \log_{10}(\tau_{0.67})$

0.29

Kaufman

Charlson et al. (92)

Stratospheric Aerosols ; Spatial-Temporal variations

○ 成層圏エアロゾルの影響：光学的厚さの時空間変動

Averaged optical thickness time series;

・平均的な光学的厚さの時系列：$\Delta\tau_{0.5} \geq 0.1$ (Index, SAGE)

Spatial distribution detection

・空間分布：AVHRRによる検知 $\Delta\tau_{0.5} \geq 0.05$

→ Ocean color sensors (OCTS, GLI) $\Delta\tau_{0.5} \geq 0.02$

・ERBE : $\Delta F_{NET} = (-11.5 \pm 4.4)\Delta\tau_{0.5} - 0.5$ (Minnis, 93)

・Surface meas. : $r_e \sim 0.6$ μm (depends on time after eruption

(Nakajima et al. '86)

IPCC 95

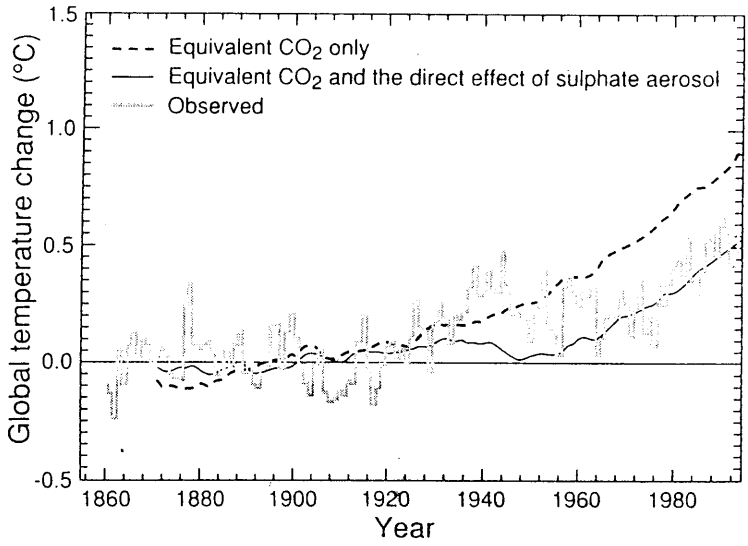

Figure 6.3: Simulated global annual mean warming from 1860 to 1990, allowing for increases in equivalent CO_2 only (dashed curve) and allowing for increases in equivalent CO_2 and the direct

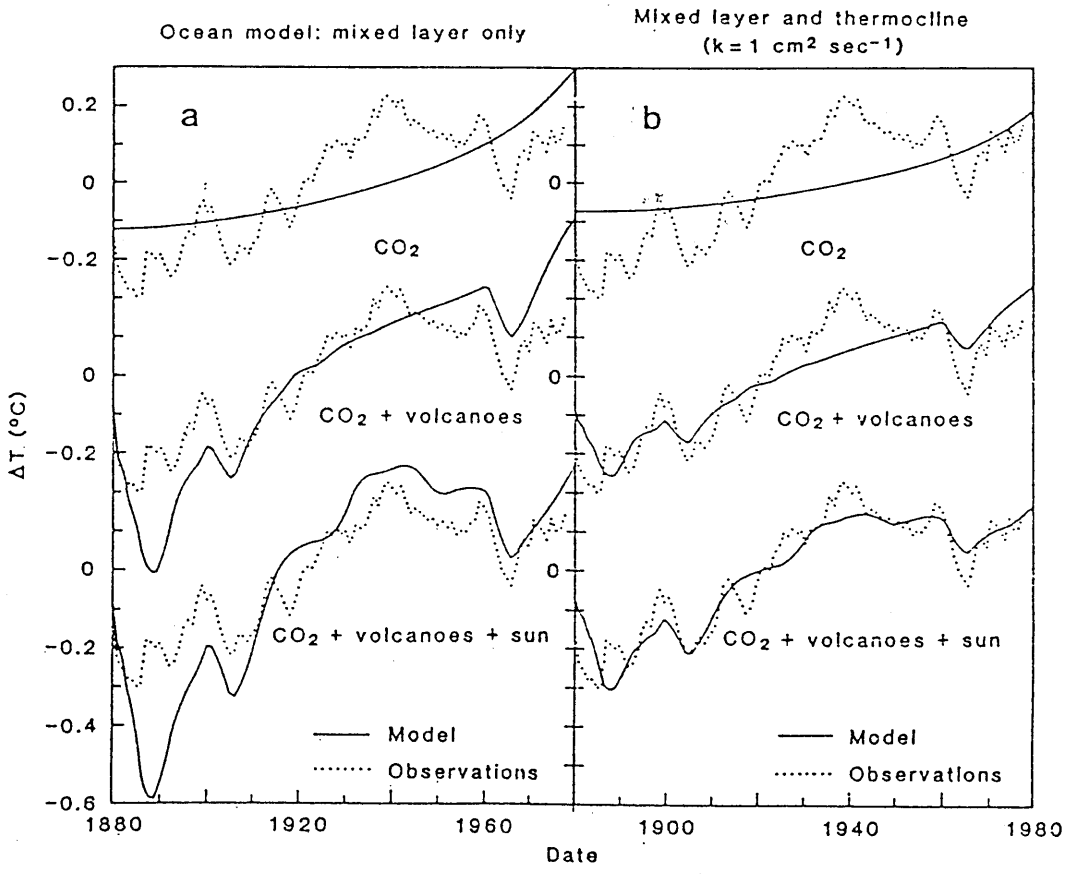

Fig. 5. Global temperature trend obtained from climate model with sensitivity 2.8°C for doubled CO_2. The results in (a) are based on a 100-m mixed-layer ocean for heat capacity; those in (b) include diffusion of heat into the thermocline to 1000 m. The forcings by CO_2, volcanoes, and the sun are based on Broecker (*25*), Lamb (*27*), and Hoyt (*48*). Mean ΔT is zero for observations and model.

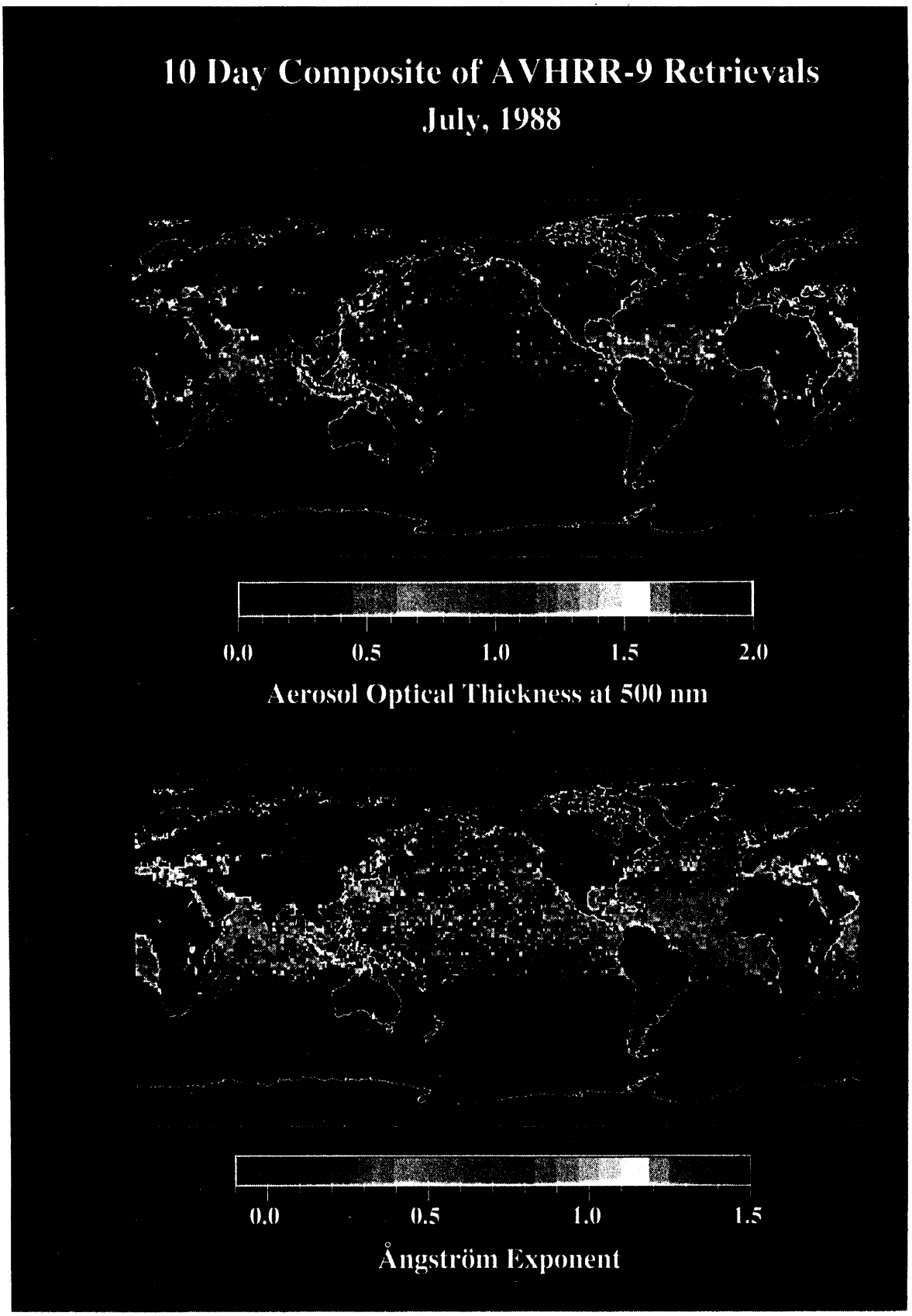
10 Day Composite of AVHRR-9 Retrievals
July, 1988
0.0
0.5
1.0
1.5
2.0
Aerosol Optical Thickness at 500 nm
0.0
0.5
1.0
1.5
Ångström Exponent

NOAA Operational Product - aerosol monthly mean

January, 1990

July, 1990

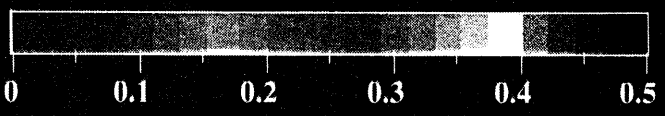

Aerosol Optical Thickness at 500 nm

Jul-Sep, 1987

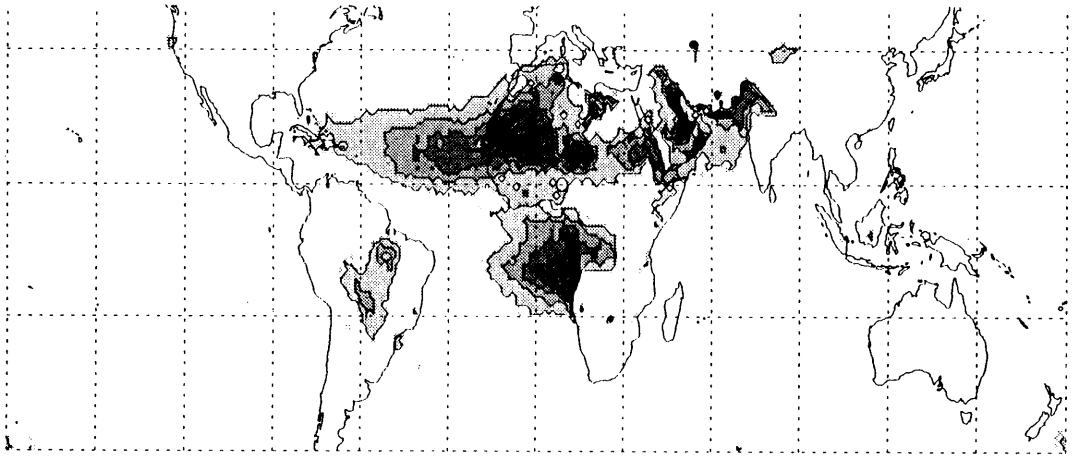

Jul-Sep, 1988

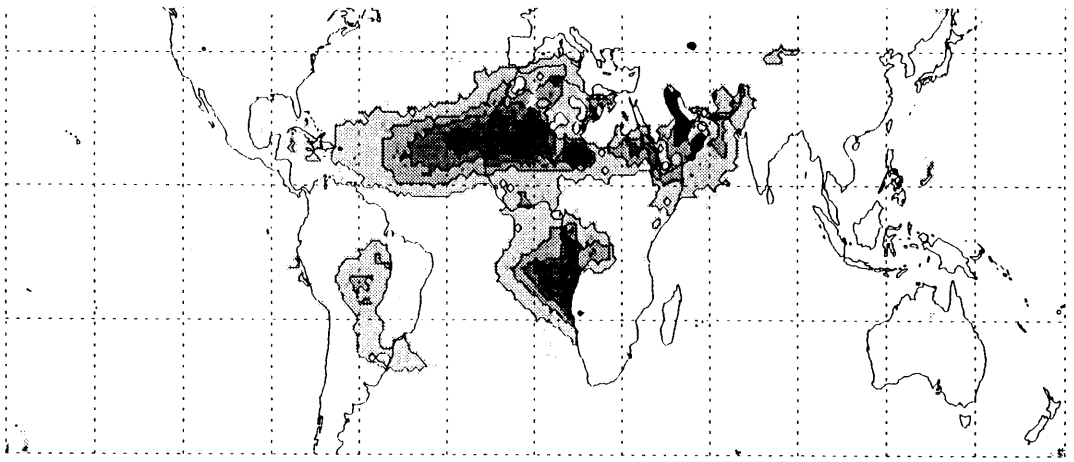

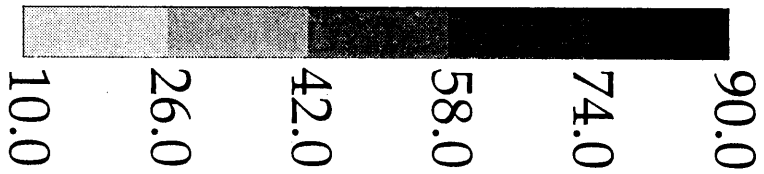

# of Days

TOMS / J. Herman Aerosol index

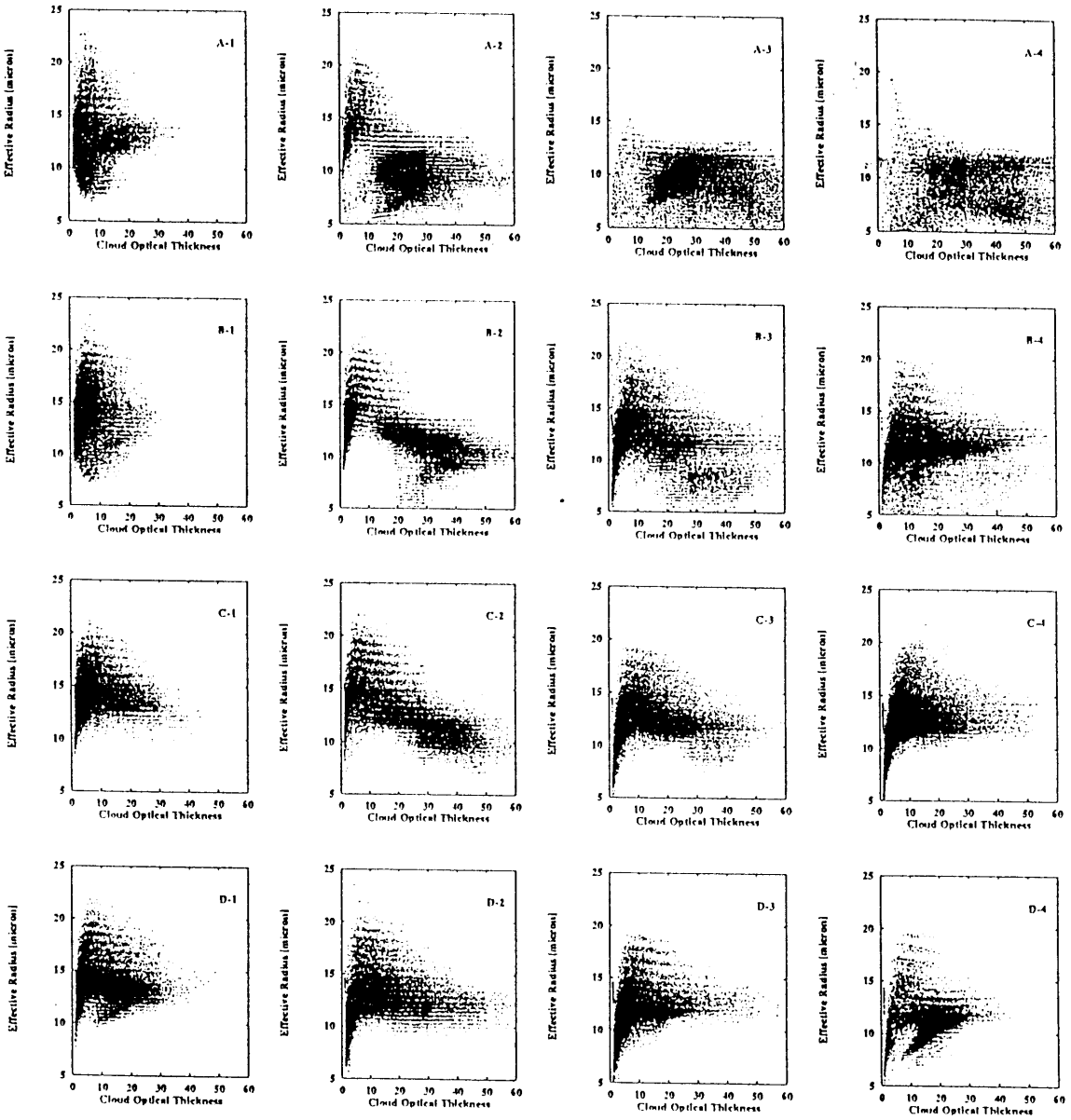

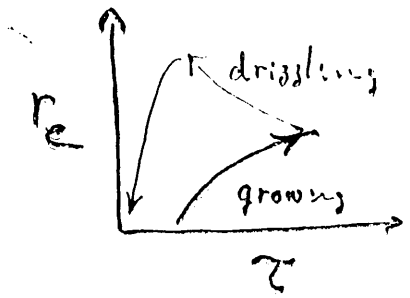

FIRE

Fig. 17

Nakajima and Nakajima

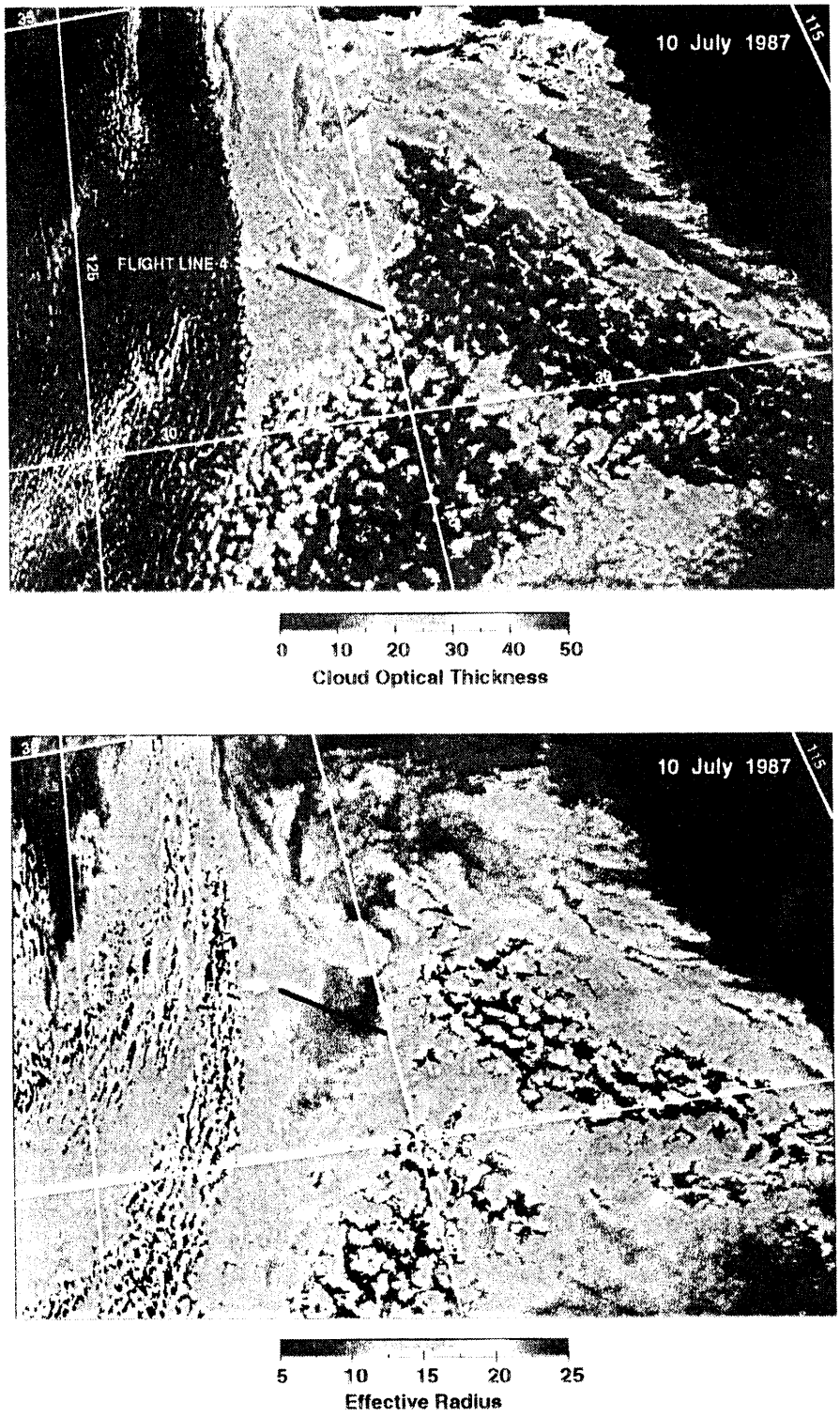

Fig. 1 AVHRR derived optical thickness and effective particle radius on 10 July 1987 in the FIRE region. The solid line labeled *flight line* is the flight leg of the ER-2 and C-131A aircrafts used in the comparison. A large difference in these parameters between left and right parts of the cloud field which were under maritime and continental airmasses, respectively. (Nakajima and Nakajima, 1995)

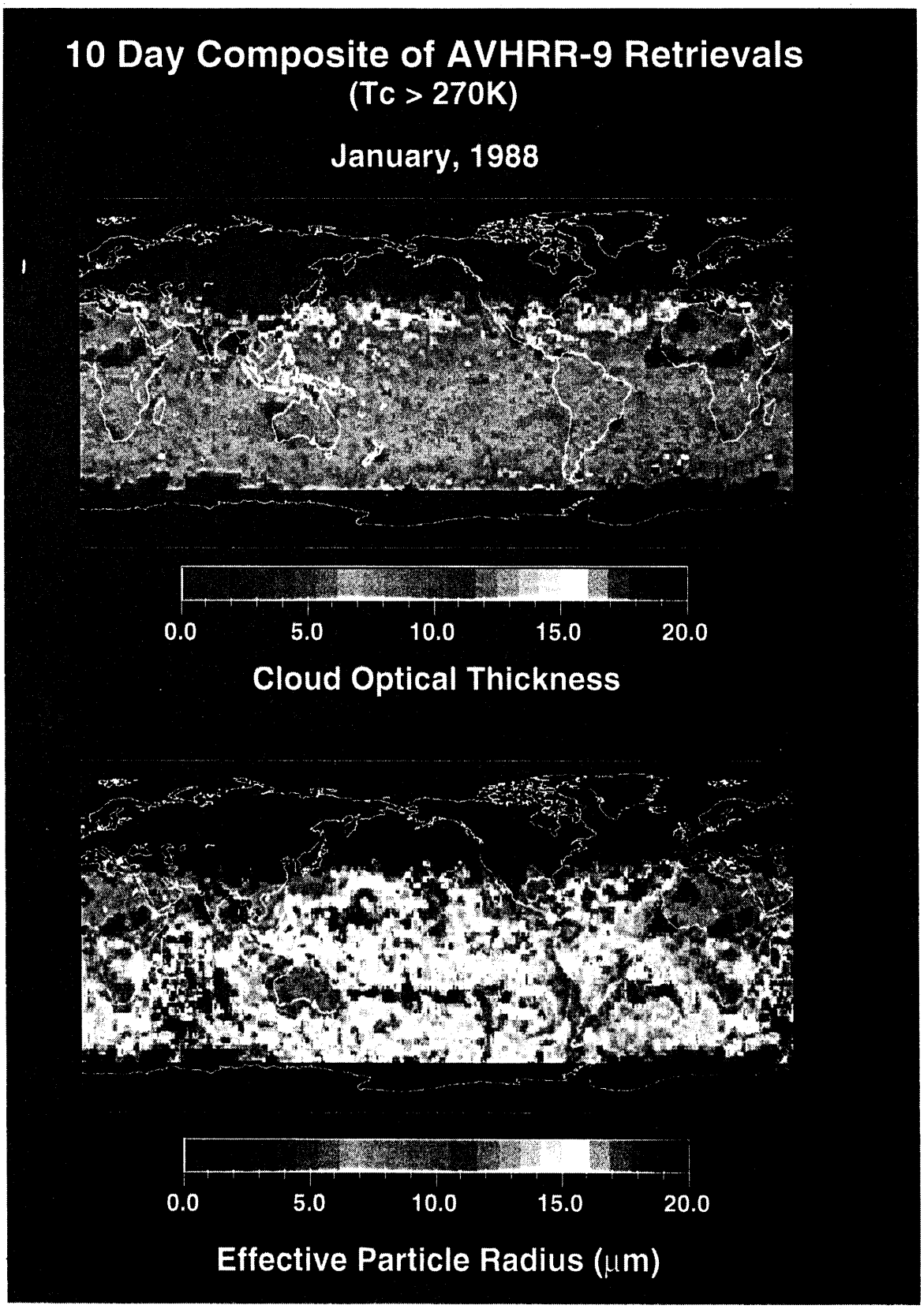
10 Day Composite of AVHRR-9 Retrievals
(Tc > 270K)
January, 1988
0.0
5.0
10.0
15.0
20.0
Cloud Optical Thickness
0.0
5.0
10.0
15.0
20.0
Effective Particle Radius (μm)

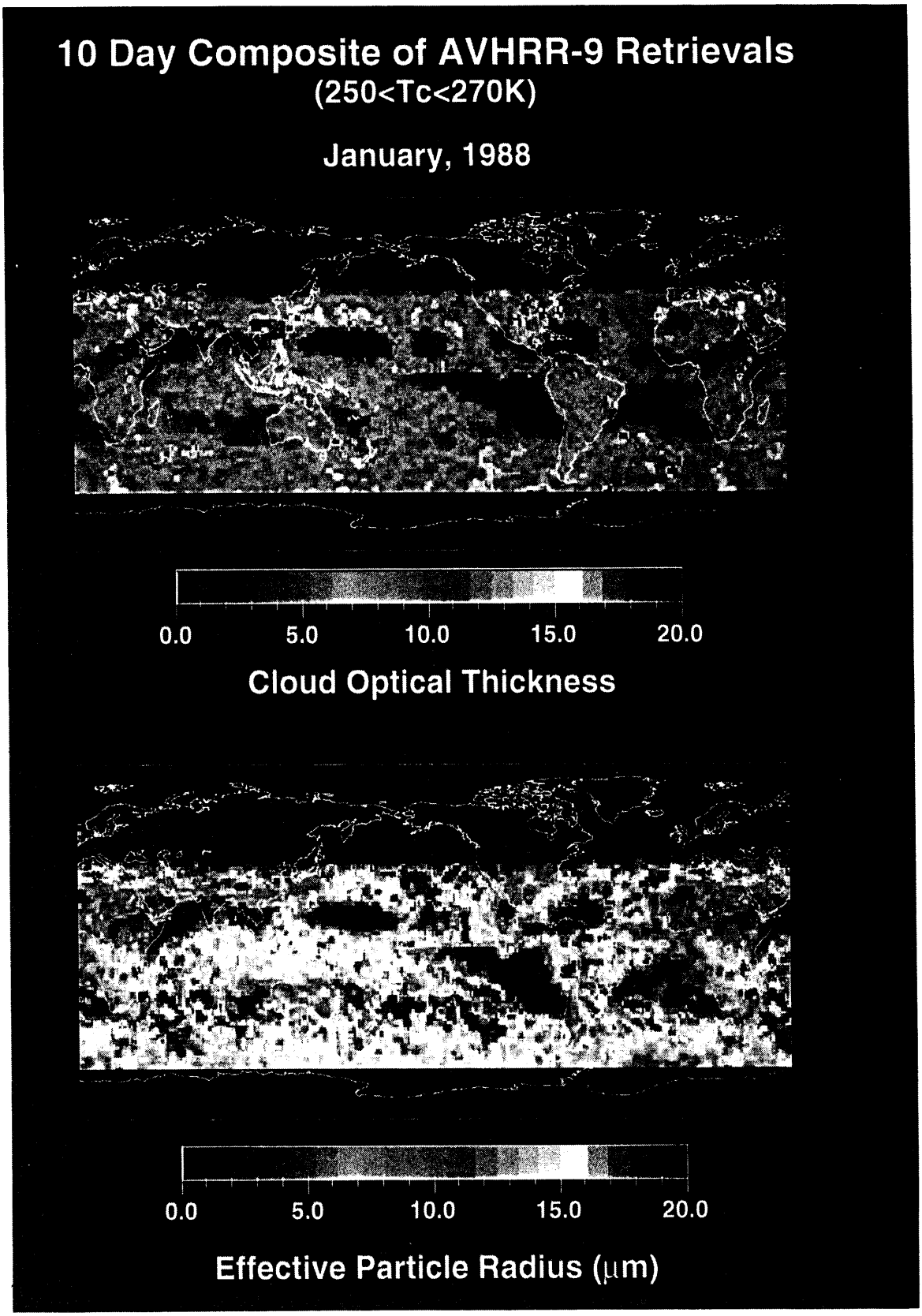
10 Day Composite of AVHRR-9 Retrievals
(250<Tc<270K)
January, 1988
0.0
5.0
10.0
15.0
20.0
Cloud Optical Thickness
0.0
5.0
10.0
15.0
20.0
Effective Particle Radius (μm)